



CHORUS

This is the accepted manuscript made available via CHORUS. The article has been published as:

Search for Resonant Top-Antitop Production in the Lepton Plus Jets Decay Mode Using the Full CDF Data Set

T. Aaltonen *et al.* (CDF Collaboration)

Phys. Rev. Lett. **110**, 121802 — Published 20 March 2013

DOI: [10.1103/PhysRevLett.110.121802](https://doi.org/10.1103/PhysRevLett.110.121802)

Search for Resonant Top-antitop Production in the Lepton Plus Jets Decay Mode Using the Full CDF Data Set

T. Aaltonen,²¹ S. Amerio,⁴⁰ D. Amidei,³² A. Anastassov,^{x, 15} A. Annovi,¹⁷ J. Antos,¹² G. Apollinari,¹⁵ J.A. Appel,¹⁵ T. Arisawa,⁵³ A. Artikov,¹³ J. Asaadi,⁴⁸ W. Ashmanskas,¹⁵ B. Auerbach,² A. Aurisano,⁴⁸ F. Azfar,³⁹ W. Badgett,¹⁵ T. Bae,²⁵ A. Barbaro-Galtieri,²⁶ V.E. Barnes,⁴⁴ B.A. Barnett,²³ P. Barria,^{hh, 42} P. Bartos,¹² M. Bauc^{ff},⁴⁰ F. Bedeschi,⁴² S. Behari,¹⁵ G. Bellettini,^{gg, 42} J. Bellinger,⁵⁵ D. Benjamin,¹⁴ A. Beretvas,¹⁵ A. Bhatti,⁴⁶ K.R. Bland,⁵ B. Blumenfeld,²³ A. Bocci,¹⁴ A. Bodek,⁴⁵ D. Bortoletto,⁴⁴ J. Boudreau,⁴³ A. Boveia,¹¹ L. Brigliadori,^{ee, 6} C. Bromberg,³³ E. Brucken,²¹ J. Budagov,¹³ H.S. Budd,⁴⁵ K. Burkett,¹⁵ G. Busetto,^{ff, 40} P. Bussey,¹⁹ P. Butti,^{gg, 42} A. Buzatu,¹⁹ A. Calamba,¹⁰ S. Camarda,⁴ M. Campanelli,²⁸ F. Canelli,^{oo, 11, 15} B. Carls,²² D. Carlsmith,⁵⁵ R. Carosi,⁴² S. Carrillo,^{m, 16} B. Casal,^{k, 9} M. Casarsa,⁴⁹ A. Castro,^{ee, 6} P. Catastini,²⁰ D. Cauz,⁴⁹ V. Cavaliere,²² M. Cavalli-Sforza,⁴ A. Cerri,^{f, 26} L. Cerrito,^{s, 28} Y.C. Chen,¹ M. Chertok,⁷ G. Chiarelli,⁴² G. Chlachidze,¹⁵ K. Cho,²⁵ D. Chokheli,¹³ M.A. Ciocci,^{hh, 42} A. Clark,¹⁸ C. Clarke,⁵⁴ M.E. Convery,¹⁵ J. Conway,⁷ M. Corbo,¹⁵ M. Cordelli,¹⁷ C.A. Cox,⁷ D.J. Cox,⁷ M. Cremonesi,⁴² D. Cruz,⁴⁸ J. Cuevas,^{z, 9} R. Culbertson,¹⁵ N. d'Ascenzo,^{w, 15} M. Datta,^{qq, 15} P. De Barbaro,⁴⁵ L. Demortier,⁴⁶ M. Deninno,⁶ F. Devoto,²¹ M. d'Errico,^{ff, 40} A. Di Canto,^{gg, 42} B. Di Ruzza,^{q, 15} J.R. Dittmann,⁵ M. D'Onofrio,²⁷ S. Donati,^{gg, 42} M. Dorigo,^{nn, 49} A. Driutti,⁴⁹ K. Ebina,⁵³ R. Edgar,³² A. Elagin,⁴⁸ R. Erbacher,⁷ S. Errede,²² B. Esham,²² R. Eusebi,⁴⁸ S. Farrington,³⁹ J.P. Fernández Ramos,²⁹ R. Field,¹⁶ G. Flanagan,^{u, 15} R. Forrest,⁷ M. Franklin,²⁰ J.C. Freeman,¹⁵ H. Frisch,¹¹ Y. Funakoshi,⁵³ A.F. Garfinkel,⁴⁴ P. Garosi,^{hh, 42} H. Gerberich,²² E. Gerchtein,¹⁵ S. Giagu,⁴⁷ V. Giakoumopoulou,³ K. Gibson,⁴³ C.M. Ginsburg,¹⁵ N. Giokaris,³ P. Giromini,¹⁷ G. Giurgiu,²³ V. Glagolev,¹³ D. Glenzinski,¹⁵ M. Gold,³⁵ D. Goldin,⁴⁸ A. Golossanov,¹⁵ G. Gomez,⁹ G. Gomez-Ceballos,³⁰ M. Goncharov,³⁰ O. González López,²⁹ I. Gorelov,³⁵ A.T. Goshaw,¹⁴ K. Goulianos,⁴⁶ E. Gramellini,⁶ S. Grinstein,⁴ C. Grosso-Pilcher,¹¹ R.C. Group,^{52, 15} J. Guimaraes da Costa,²⁰ S.R. Hahn,¹⁵ J.Y. Han,⁴⁵ F. Happacher,¹⁷ K. Hara,⁵⁰ M. Hare,⁵¹ R.F. Harr,⁵⁴ T. Harrington-Taber,^{n, 15} K. Hatakeyama,⁵ C. Hays,³⁹ J. Heinrich,⁴¹ M. Herndon,⁵⁵ A. Hocker,¹⁵ Z. Hong,⁴⁸ W. Hopkins,^{g, 15} S. Hou,¹ R.E. Hughes,³⁶ U. Husemann,⁵⁶ M. Hussein,³³ J. Huston,³³ G. Introzzi,^{mm, 42} M. Iori,^{jj, 47} A. Ivanov,^{p, 7} E. James,¹⁵ D. Jang,¹⁰ B. Jayatilaka,¹⁵ E.J. Jeon,²⁵ S. Jindariani,¹⁵ M. Jones,⁴⁴ K.K. Joo,²⁵ S.Y. Jun,¹⁰ T.R. Junk,¹⁵ M. Kambeitz,²⁴ T. Kamon,^{25, 48} P.E. Karchin,⁵⁴ A. Kasmi,⁵ Y. Kato,^{o, 38} W. Ketchum,^{rr, 11} J. Keung,⁴¹ B. Kilminster,^{oo, 15} D.H. Kim,²⁵ H.S. Kim,²⁵ J.E. Kim,²⁵ M.J. Kim,¹⁷ S.B. Kim,²⁵ S.H. Kim,⁵⁰ Y.K. Kim,¹¹ Y.J. Kim,²⁵ N. Kimura,⁵³ M. Kirby,¹⁵ K. Knoepfel,¹⁵ K. Kondo,^{*, 53} D.J. Kong,²⁵ J. Konigsberg,¹⁶ A.V. Kotwal,¹⁴ M. Kreps,²⁴ J. Kroll,⁴¹ M. Kruse,¹⁴ T. Kuhr,²⁴ M. Kurata,⁵⁰ A.T. Laasanen,⁴⁴ S. Lammel,¹⁵ M. Lancaster,²⁸ K. Lannon,^{y, 36} G. Latino,^{hh, 42} H.S. Lee,²⁵ J.S. Lee,²⁵ S. Leo,⁴² S. Leone,⁴² J.D. Lewis,¹⁵ A. Limosani,^{t, 14} E. Lipeles,⁴¹ H. Liu,⁵² Q. Liu,⁴⁴ T. Liu,¹⁵ S. Lockwitz,⁵⁶ A. Loginov,⁵⁶ D. Lucchesi,^{ff, 40} J. Lueck,²⁴ P. Lujan,²⁶ P. Lukens,¹⁵ G. Lungu,⁴⁶ J. Lys,²⁶ R. Lysak,^{e, 12} R. Madrak,¹⁵ P. Maestro,^{hh, 42} S. Malik,⁴⁶ G. Manca,^{a, 27} A. Manousakis-Katsikakis,³ F. Margaroli,⁴⁷ P. Marino,^{ii, 42} M. Martínez,⁴ K. Matera,²² M.E. Mattson,⁵⁴ A. Mazzacane,¹⁵ P. Mazzanti,⁶ R. McNulty,^{j, 27} A. Mehta,²⁷ P. Mehtala,²¹ C. Mesropian,⁴⁶ T. Miao,¹⁵ D. Mietlicki,³² A. Mitra,¹ H. Miyake,⁵⁰ S. Moed,¹⁵ N. Moggi,⁶ C.S. Moon,^{aa, 15} R. Moore,^{pp, 15} M.J. Morello,^{ii, 42} A. Mukherjee,¹⁵ Th. Muller,²⁴ P. Murat,¹⁵ M. Mussini,^{ee, 6} J. Nachtman,^{n, 15} Y. Nagai,⁵⁰ J. Naganoma,⁵³ I. Nakano,³⁷ A. Napier,⁵¹ J. Nett,⁴⁸ C. Neu,⁵² T. Nigmanov,⁴³ L. Nodulman,² S.Y. Noh,²⁵ O. Norriella,²² L. Oakes,³⁹ S.H. Oh,¹⁴ Y.D. Oh,²⁵ I. Oksuzian,⁵² T. Okusawa,³⁸ R. Orava,²¹ L. Ortolan,⁴ C. Pagliarone,⁴⁹ E. Palencia,^{f, 9} P. Palmi,³⁵ V. Papadimitriou,¹⁵ W. Parker,⁵⁵ G. Pauletta,^{kk, 49} M. Paulini,¹⁰ C. Paus,³⁰ T.J. Phillips,¹⁴ G. Piacentino,⁴² E. Pianori,⁴¹ J. Pilot,³⁶ K. Pitts,²² C. Plager,⁸ L. Pondrom,⁵⁵ S. Poprocki,^{g, 15} K. Potamianos,²⁶ F. Prokoshin,^{cc, 13} A. Pranko,²⁶ F. Ptohos,^{h, 17} G. Punzi,^{gg, 42} N. Ranjan,⁴⁴ I. Redondo Fernández,²⁹ P. Renton,³⁹ M. Rescigno,⁴⁷ T. Riddick,²⁸ F. Rimondi,^{*, 6} L. Ristori,^{42, 15} A. Robson,¹⁹ T. Rodriguez,⁴¹ S. Rolli,^{i, 51} M. Ronzani,^{gg, 42} R. Roser,¹⁵ J.L. Rosner,¹¹ F. Ruffini,^{hh, 42} A. Ruiz,⁹ J. Russ,¹⁰ V. Rusu,¹⁵ A. Safonov,⁴⁸ W.K. Sakumoto,⁴⁵ Y. Sakurai,⁵³ L. Santi,^{kk, 49} K. Sato,⁵⁰ V. Saveliev,^{w, 15} A. Savoy-Navarro,^{aa, 15} P. Schlabach,¹⁵ E.E. Schmidt,¹⁵ T. Schwarz,³² L. Scodellaro,⁹ F. Scuri,⁴² S. Seidel,³⁵ Y. Seiya,³⁸ A. Semenov,¹³ F. Sforza,^{gg, 42} S.Z. Shalhout,⁷ T. Shears,²⁷ P.F. Shepard,⁴³ M. Shimojima,^{v, 50} M. Shochet,¹¹ I. Shreyber-Tecker,³⁴ A. Simonenko,¹³ P. Sinervo,³¹ K. Sliwa,⁵¹ J.R. Smith,⁷ F.D. Snider,¹⁵ V. Sorin,⁴ H. Song,⁴³ M. Stancari,¹⁵ R. St. Denis,¹⁹ B. Stelzer,³¹ O. Stelzer-Chilton,³¹ D. Stentz,^{x, 15} J. Strologas,³⁵ Y. Sudo,⁵⁰ A. Sukhanov,¹⁵ I. Suslov,¹³ K. Takemasa,⁵⁰ Y. Takeuchi,⁵⁰ J. Tang,¹¹ M. Tecchio,³² P.K. Teng,¹ J. Thom,^{g, 15} E. Thomson,⁴¹ V. Thukral,⁴⁸ D. Töback,⁴⁸ S. Tokar,¹² K. Tollefson,³³ T. Tomura,⁵⁰ D. Tonelli,^{f, 15} S. Torre,¹⁷

D. Torretta,¹⁵ P. Totaro,⁴⁰ M. Trovato^{ii, 42} F. Ukegawa,⁵⁰ S. Uozumi,²⁵ F. Vázquez^{m, 16} G. Velev,¹⁵ C. Vellidis,¹⁵ C. Vernieri^{ii, 42} M. Vidal,⁴⁴ R. Vilar,⁹ J. Vizán^{ll, 9} M. Vogel,³⁵ G. Volpi,¹⁷ P. Wagner,⁴¹ R. Wallny,⁸ S.M. Wang,¹ A. Warburton,³¹ D. Waters,²⁸ W.C. Wester III,¹⁵ D. Whiteson^{b, 41} A.B. Wicklund,² S. Wilbur,¹¹ H.H. Williams,⁴¹ J.S. Wilson,³² P. Wilson,¹⁵ B.L. Winer,³⁶ P. Wittich^{g, 15} S. Wolbers,¹⁵ H. Wolfe,³⁶ T. Wright,³² X. Wu,¹⁸ Z. Wu,⁵ K. Yamamoto,³⁸ D. Yamato,³⁸ T. Yang,¹⁵ U.K. Yang^{r, 11} Y.C. Yang,²⁵ W.-M. Yao,²⁶ G.P. Yeh,¹⁵ K. Yi^{n, 15} J. Yoh,¹⁵ K. Yorita,⁵³ T. Yoshida^{l, 38} G.B. Yu,¹⁴ I. Yu,²⁵ A.M. Zanetti,⁴⁹ Y. Zeng,¹⁴ C. Zhou,¹⁴ and S. Zucchelli^{ee6}
(CDF Collaboration[†])

The CDF Collaboration⁵⁷

- ¹*Institute of Physics, Academia Sinica, Taipei, Taiwan 11529, Republic of China*
²*Argonne National Laboratory, Argonne, Illinois 60439, USA*
³*University of Athens, 157 71 Athens, Greece*
⁴*Institut de Física d'Altes Energies, ICREA, Universitat Autònoma de Barcelona, E-08193, Bellaterra (Barcelona), Spain*
⁵*Baylor University, Waco, Texas 76798, USA*
⁶*Istituto Nazionale di Fisica Nucleare Bologna, ^{ee}University of Bologna, I-40127 Bologna, Italy*
⁷*University of California, Davis, Davis, California 95616, USA*
⁸*University of California, Los Angeles, Los Angeles, California 90024, USA*
⁹*Instituto de Física de Cantabria, CSIC-University of Cantabria, 39005 Santander, Spain*
¹⁰*Carnegie Mellon University, Pittsburgh, Pennsylvania 15213, USA*
¹¹*Enrico Fermi Institute, University of Chicago, Chicago, Illinois 60637, USA*
¹²*Comenius University, 842 48 Bratislava, Slovakia; Institute of Experimental Physics, 040 01 Kosice, Slovakia*
¹³*Joint Institute for Nuclear Research, RU-141980 Dubna, Russia*
¹⁴*Duke University, Durham, North Carolina 27708, USA*
¹⁵*Fermi National Accelerator Laboratory, Batavia, Illinois 60510, USA*
¹⁶*University of Florida, Gainesville, Florida 32611, USA*
¹⁷*Laboratori Nazionali di Frascati, Istituto Nazionale di Fisica Nucleare, I-00044 Frascati, Italy*
¹⁸*University of Geneva, CH-1211 Geneva 4, Switzerland*
¹⁹*Glasgow University, Glasgow G12 8QQ, United Kingdom*
²⁰*Harvard University, Cambridge, Massachusetts 02138, USA*
²¹*Division of High Energy Physics, Department of Physics, University of Helsinki and Helsinki Institute of Physics, FIN-00014, Helsinki, Finland*
²²*University of Illinois, Urbana, Illinois 61801, USA*
²³*The Johns Hopkins University, Baltimore, Maryland 21218, USA*
²⁴*Institut für Experimentelle Kernphysik, Karlsruhe Institute of Technology, D-76131 Karlsruhe, Germany*
²⁵*Center for High Energy Physics: Kyungpook National University, Daegu 702-701, Korea; Seoul National University, Seoul 151-742, Korea; Sungkyunkwan University, Suwon 440-746, Korea; Korea Institute of Science and Technology Information, Daejeon 305-806, Korea; Chonnam National University, Gwangju 500-757, Korea; Chonbuk National University, Jeonju 561-756, Korea; Ewha Womans University, Seoul, 120-750, Korea*
²⁶*Ernest Orlando Lawrence Berkeley National Laboratory, Berkeley, California 94720, USA*
²⁷*University of Liverpool, Liverpool L69 7ZE, United Kingdom*
²⁸*University College London, London WC1E 6BT, United Kingdom*
²⁹*Centro de Investigaciones Energéticas Medioambientales y Tecnológicas, E-28040 Madrid, Spain*
³⁰*Massachusetts Institute of Technology, Cambridge, Massachusetts 02139, USA*
³¹*Institute of Particle Physics: McGill University, Montréal, Québec H3A 2T8, Canada; Simon Fraser University, Burnaby, British Columbia V5A 1S6, Canada; University of Toronto, Toronto, Ontario M5S 1A7, Canada; and TRIUMF, Vancouver, British Columbia V6T 2A3, Canada*
³²*University of Michigan, Ann Arbor, Michigan 48109, USA*
³³*Michigan State University, East Lansing, Michigan 48824, USA*
³⁴*Institution for Theoretical and Experimental Physics, ITEP, Moscow 117259, Russia*
³⁵*University of New Mexico, Albuquerque, New Mexico 87131, USA*
³⁶*The Ohio State University, Columbus, Ohio 43210, USA*
³⁷*Okayama University, Okayama 700-8530, Japan*
³⁸*Osaka City University, Osaka 588, Japan*
³⁹*University of Oxford, Oxford OX1 3RH, United Kingdom*
⁴⁰*Istituto Nazionale di Fisica Nucleare, Sezione di Padova-Trento, ^{ff}University of Padova, I-35131 Padova, Italy*
⁴¹*University of Pennsylvania, Philadelphia, Pennsylvania 19104, USA*

- ⁴²*Istituto Nazionale di Fisica Nucleare Pisa*, ⁹⁹*University of Pisa*,
^{hh}*University of Siena* and ⁱⁱ*Scuola Normale Superiore, I-56127 Pisa*,
Italy, ^{mm}*INFN Pavia and University of Pavia, I-27100 Pavia, Italy*
⁴³*University of Pittsburgh, Pittsburgh, Pennsylvania 15260, USA*
⁴⁴*Purdue University, West Lafayette, Indiana 47907, USA*
⁴⁵*University of Rochester, Rochester, New York 14627, USA*
⁴⁶*The Rockefeller University, New York, New York 10065, USA*
⁴⁷*Istituto Nazionale di Fisica Nucleare, Sezione di Roma 1*,
^{jj}*Sapienza Università di Roma, I-00185 Roma, Italy*
⁴⁸*Texas A&M University, College Station, Texas 77843, USA*
⁴⁹*Istituto Nazionale di Fisica Nucleare Trieste/Udine; ⁿⁿUniversity of Trieste*,
I-34127 Trieste, Italy; ^{kk}*University of Udine, I-33100 Udine, Italy*
⁵⁰*University of Tsukuba, Tsukuba, Ibaraki 305, Japan*
⁵¹*Tufts University, Medford, Massachusetts 02155, USA*
⁵²*University of Virginia, Charlottesville, Virginia 22906, USA*
⁵³*Waseda University, Tokyo 169, Japan*
⁵⁴*Wayne State University, Detroit, Michigan 48201, USA*
⁵⁵*University of Wisconsin, Madison, Wisconsin 53706, USA*
⁵⁶*Yale University, New Haven, Connecticut 06520, USA*
⁵⁷URL <http://www-cdf.fnal.gov>

This Letter reports a search for a narrow resonant state decaying into two W bosons and two b quarks where one W boson decays leptonically and the other decays into a quark-antiquark pair. The search is particularly sensitive to top-antitop resonant production. We use the full data sample of proton-antiproton collisions at a center-of-mass energy of 1.96 TeV collected by the CDF II detector at the Fermilab Tevatron, corresponding to an integrated luminosity of 9.45 fb^{-1} . No evidence for resonant production is found and upper limits on the production cross section times branching ratio for a narrow resonant state are extracted. Within a specific benchmark model, we exclude a Z' boson with mass, $M_{Z'}$, below $915 \text{ GeV}/c^2$ decaying into a top-antitop pair at the 95% credibility level assuming a Z' boson decay width of $\Gamma_{Z'} = 0.012 M_{Z'}$. This is the most sensitive search for a narrow $q\bar{q}$ -initiated $t\bar{t}$ resonance in the mass region below $750 \text{ GeV}/c^2$.

PACS numbers: 13.85.Rm, 14.65.Ha, 14.70.Pw, 14.80.Tt

*Deceased

†With visitors from ^a*Istituto Nazionale di Fisica Nucleare, Sezione di Cagliari, 09042 Monserrato (Cagliari), Italy*, ^b*University of California Irvine, Irvine, CA 92697, USA*, ^c*Institute of Physics, Academy of Sciences of the Czech Republic, 182 21, Czech Republic*, ^f*CERN, CH-1211 Geneva, Switzerland*, ^g*Cornell University, Ithaca, NY 14853, USA*, ^h*University of Cyprus, Nicosia CY-1678, Cyprus*, ⁱ*Office of Science, U.S. Department of Energy, Washington, DC 20585, USA*, ^j*University College Dublin, Dublin 4, Ireland*, ^k*ETH, 8092 Zürich, Switzerland*, ^l*University of Fukui, Fukui City, Fukui Prefecture, Japan 910-0017*, ^m*Universidad Iberoamericana, Lomas de Santa Fe, México, C.P. 01219, Distrito Federal*, ⁿ*University of Iowa, Iowa City, IA 52242, USA*, ^o*Kinki University, Higashi-Osaka City, Japan 577-8502*, ^p*Kansas State University, Manhattan, KS 66506, USA*, ^q*Brookhaven National Laboratory, Upton, NY 11973, USA*, ^r*University of Manchester, Manchester M13 9PL, United Kingdom*, ^s*Queen Mary, University of London, London, E1 4NS, United Kingdom*, ^t*University of Melbourne, Victoria 3010, Australia*, ^u*Muons, Inc., Batavia, IL 60510, USA*, ^v*Nagasaki Institute of Applied Science, Nagasaki 851-0193, Japan*, ^w*National Research Nuclear University, Moscow 115409, Russia*, ^x*Northwestern University, Evanston, IL 60208, USA*, ^y*University of Notre Dame, Notre Dame, IN 46556, USA*, ^z*Universidad de Oviedo, E-33007 Oviedo, Spain*, ^{aa}*CNRS-IN2P3, Paris, F-75205 France*, ^{cc}*Universidad Tecnica Federico Santa Maria, 110v Valparaiso, Chile*, ^{dd}*Yarmouk University, Irbid 211-63, Jordan*, ^{ll}*Universite catholique de Louvain, 1348 Louvain-La-Neuve, Belgium*, ^{oo}*University of Zürich, 8006 Zürich, Switzerland*,

The large mass of the top quark, compared to that of the other fundamental particles, gives it a special position within the standard model (SM). Since its discovery [1], the top quark has played an important role in theoretical extensions beyond the standard model (BSM) [2]. Recently, renewed interest has been directed toward searches including top quark final states for BSM physics due to discrepancies reported in the $t\bar{t}$ forward-backward asymmetry [3, 4]. Moreover, the most recent search for resonant $t\bar{t}$ production from D0 [5] reports an approximately 2σ excess of events at resonant-mass values around $950 \text{ GeV}/c^2$. Many BSM theories [6–10] predict heavy resonances that add a resonant component to the SM $t\bar{t}$ production mechanism.

Top quarks decay via the weak interaction, nearly always into a W boson and a b quark. The W boson then decays into lighter fermion-antifermion pair [11]. We search for resonant production of top quark pairs followed by decays into a final state with one charged

^{pp}Massachusetts General Hospital and Harvard Medical School, Boston, MA 02114 USA, ^{qq}Hampton University, Hampton, VA 23668, USA, ^{rr}Los Alamos National Laboratory, Los Alamos, NM 87544, USA

lepton (electron or muon) and multiple jets, where one of the W bosons decays leptonically and the other W boson decays hadronically. This lepton+jets channel features a distinctive final state due to the presence of a charged lepton and has a branching ratio of 29% [12].

Unlike previous searches at CDF [13–16], we do not apply constraints based on the presence of top quarks in the event. While we focus the discussion on $t\bar{t}$ resonances, we construct the top-antitop mass $M_{t\bar{t}}$ used as a final search discriminant by taking the invariant mass of all objects (lepton, jets, and missing E_T) in the event including those that may not originate from top quark production. Other than the event selection defined below, which provides a sample primarily composed of $t\bar{t}$ events, there are no requirements that the event be consistent with $t\bar{t}$ production. This results in a more general search that is sensitive not only to $t\bar{t}$, but also to any heavy narrow resonance decaying into a final state with a W boson and three or more jets with one or two jets originating from a b quark.

As a benchmark model, we consider a specific SM extension, topcolor-assisted technicolor [17, 18]. This model explains the large mass of the top quark through the introduction of new strong dynamics and also predicts a vector particle (Z' boson), which couples primarily to the third generation of quarks and has no significant couplings to leptons. The existence of a narrow-width Z' boson resonance ($\Gamma_{Z'} = 0.012 M_{Z'}$) decaying to $t\bar{t}$ pairs, using the leptophobic topcolor model [18, 19], has been searched for both by the CDF [13–16] and D0 [5, 20, 21] experiments at the Tevatron, and also by the ATLAS [22–24] and CMS [25, 26] experiments at the LHC. For resonance searches at the highest masses, the LHC experiments have superior sensitivity to the Tevatron due to the higher center-of-mass energy. However, in the lower-mass regions ($m_{Z'} < 750 \text{ GeV}/c^2$) the Tevatron experiments have competitive sensitivity in searches for particles produced in $q\bar{q}$ -initiated states, such as the Z' boson. While the production rate for the main background from SM $t\bar{t}$ is approximately 25 times larger at a center-of-mass energy of 7 TeV, no valence antiquarks are available in the LHC pp collisions, so the signal production rate increases by a smaller factor relative to the $p\bar{p}$ collisions of the Tevatron (between four and eight in the lower-mass region).

The collision events discussed in this Letter were produced at the Tevatron $p\bar{p}$ collider at a center-of-mass energy of 1.96 TeV and were recorded by the CDF II detector [27]. The data sample corresponds to the full data set of the Tevatron, which comes from an integrated luminosity of 9.45 fb^{-1} . The CDF II detector consists of high-precision tracking systems for vertex and charged-particle track reconstruction, surrounded by electromagnetic and hadronic calorimeters for energy measurement, and muon subsystems outside the calorimeter for muon detection. CDF II uses a cylindrical coordinate system

with azimuthal angle ϕ , polar angle θ measured with respect to the positive z direction along the proton beam, and the distance r measured from the beamline. The pseudorapidity, transverse energy, and transverse momentum are defined as $\eta = -\ln[\tan(\frac{\theta}{2})]$, $E_T = E \sin \theta$, and $p_T = p \sin \theta$, respectively, where E and p are the energy and momentum of an outgoing particle. The missing transverse energy \cancel{E}_T is defined by $\cancel{E}_T = -\sum_i E_T^i \hat{n}_i$, where \hat{n}_i is a unit vector perpendicular to the beam axis that points to the i th calorimeter tower ($\cancel{E}_T = |\cancel{E}_T|$).

The event selection and background estimation methods summarized below closely follow those that were employed in the observation of single top quark production [28] and in the search for the Higgs boson in the $WH \rightarrow \ell\nu b\bar{b}$ final state [29]. The main difference is that the single top and WH analyses select events consistent with W + two or three jets and the current search requires three or more jets.

The data were collected using online event selections (triggers) requiring one of the following energetic-lepton signatures: a high transverse momentum (p_T) electron candidate, a high- p_T muon candidate, or large \cancel{E}_T . Significant \cancel{E}_T can be produced when the neutrino from a leptonic W boson decay escapes detection.

Candidate events are selected by requiring a lepton candidate with $p_T^\ell > 20 \text{ GeV}/c$, $\cancel{E}_T > 20 \text{ GeV}$, and three or more jets with $|\eta| < 2.0$ and $E_T > 20 \text{ GeV}$ after correcting the jet energies for instrumental effects [30, 31]. One or two jets must be identified as being likely to have originated from a b quark according to the SECVTX [32] algorithm. This algorithm searches in the jet for a secondary vertex which results from the displaced decay of B hadrons. Events are rejected if more than one lepton candidate is reconstructed, or if they are kinematically inconsistent with leptonic W boson decays [33]. Events with severely misreconstructed jets or leptons are removed based on angular correlations between the jet or lepton candidate and the \cancel{E}_T .

Models for background processes are derived from a mixture of simulation and data-driven techniques [28]. Important backgrounds in this final state include SM $t\bar{t}$ production and other processes that include a W or Z boson in association with three or more jets. The events can include true b -quark jets, as in W boson + $b\bar{b}j$ events, or jets that have been misidentified as b -quark jets, such as in W boson + $c\bar{c}j$ and W boson + $j\bar{j}j$ events, where j refers to jets not originating from heavy-flavor quarks. Multijet events without W bosons also contribute to the sample composition. Additional small background contributions are included from Z boson production with additional jets, diboson production, and single top quark production.

The expected rate for the SM $t\bar{t}$ background is taken to be $7.04 \pm 0.70 \text{ pb}$ [34] as calculated at approximate next-to-next-to-leading order using MSTW 2008 parton distribution functions [35]. In order to predict the acceptance

Process	3-jet events	≥ 4 -jet events
$t\bar{t}$	1930 ± 200	2570 ± 270
W/Z boson + jets	2280 ± 610	570 ± 190
Multijets	150 ± 60	130 ± 100
Total background	4360 ± 870	3270 ± 560
Observed	4254	3049

TABLE I: Summary of the background prediction and observed data for three-jet and four-or-more-jet events. The uncertainties include statistical and systematic contributions.

for non-resonant SM $t\bar{t}$ events and their kinematic distributions, we use a sample of Monte Carlo (MC) events generated using POWHEG [36] and assuming a top quark mass of $172.5 \text{ GeV}/c^2$ with parton showering provided by PYTHIA [38] followed by simulation of the CDF II detector [39, 40]. The detection efficiency predicted by the simulation is corrected based on measurements using data for lepton identification, trigger efficiencies, and b -jet tagging efficiencies. The normalization for the QCD multijet and W boson + jet processes is obtained from a fit to the \cancel{E}_T distribution. The background from events with mistakenly b -tagged light-flavor jets, W boson + jjj for example, is estimated by measuring the rate of such mistags in multijet data [32] and applying this rate to the W boson + jets data samples before b tagging. The contribution from true heavy-flavor production in the W boson + jets event sample is determined from measurements of the heavy-flavor event fraction in a W boson + 1 jet sample that is independent of the sample used in the resonance search. We model the kinematic distributions of W boson + jets events using a combination of ALPGEN [41] matrix-element generation and PYTHIA parton showering. The QCD multijet background is modeled using a sample of collision events in which one of the lepton identification requirements is inverted to obtain an enriched sample of QCD multijet events.

The background predictions are summarized in Table I. In this table and the following figures we have divided the sample into events that include three jets and events that include four or more jets. For the statistical interpretation of the data we further subdivide the events based on the number of b -tagged jets (one or two b tags) and based on the lepton type (lepton types that can be directly identified by the trigger, or leptons in events selected with the \cancel{E}_T -based trigger), yielding eight independent channels used to search for a resonance in the $M_{t\bar{t}}$ distributions. The sensitivity of the search benefits from this subdivision because the search subchannels have different background compositions, signal-to-background ratios, and invariant mass resolutions.

We use the invariant mass of all reconstructed objects in the event to discriminate between SM background and

Z' boson signal events. For each event we calculate $M_{t\bar{t}}$ using the momenta of the three or more jets, the charged lepton, and the neutrino. The transverse momentum of the neutrino is estimated from the \cancel{E}_T . However, because the z -component of the momenta of the scattering partons from the $p\bar{p}$ collision is unknown, the final-state reconstructed energy need not be balanced in the z direction. The longitudinal component of the neutrino momentum (p_z^ν) is determined by solving $M_W^2 = (p^l + p^\nu)^2$, where M_W , p^l , and p^ν are the W boson mass, the lepton momentum, and the neutrino momentum, respectively. The smaller solution of the resulting quadratic equation is chosen for the p_z^ν . If there is no real solution we set $p_z^\nu = 0$. This approach is found to select the correct p_z^ν in about 70% of simulated $t\bar{t}$ events.

For the benchmark model, the Z' boson cross sections times branching fraction are based on leading-order predictions from Ref. [19] with an additional scaling factor of 1.3 applied to account for next-to-leading-order effects [42]. Signal Z' boson events are modeled with simulated events generated by PYTHIA in order to study the signal acceptance and to predict the $M_{t\bar{t}}$ distributions.

A total of 4254 (3049) events survive the selection criteria for the three-jet (four-or-more-jet) category. The SM $t\bar{t}$ contribution is estimated to be 43% (78%) for three-jet (four-or-more-jet) events. The remaining events are contributed primarily from the W boson + jet and QCD multijet processes plus a potential signal contribution from Z' boson events. The $M_{t\bar{t}}$ distributions for the background model and events observed in the data are shown in Fig. 1. We fit the $M_{t\bar{t}}$ distributions to what is observed in the data, allowing the background predictions to float within their systematic uncertainties. The $M_{t\bar{t}}$ distribution for the Z' boson signal for the $600 \text{ GeV}/c^2$ mass hypothesis is also included in Fig. 1.

We calculate a Bayesian credibility level (C.L.) limit on resonant $t\bar{t}$ production for each mass hypothesis based on the binned observed $M_{t\bar{t}}$ spectrum using the combined likelihood which includes the priors, $\pi(\vec{\theta})$, on the systematic uncertainties, $\vec{\theta}$:

$$\mathcal{L}(R, \vec{s}, \vec{b} | \vec{n}, \vec{\theta}) \times \pi(\vec{\theta}) = \prod_{i=1}^{N_C} \prod_{j=1}^{N_{\text{bins}}} \mu_{ij}^{n_{ij}} \frac{e^{-\mu_{ij}}}{n_{ij}!} \times \prod_{k=1}^{n_{\text{sys}}} e^{-\theta_k^2/2}. \quad (1)$$

In this expression, the first product is over the eight channels, N_C , we consider in this analysis. The second product is over histogram bins containing n_{ij} events. The predictions for the bin contents are $\mu_{ij} = R \times s_{ij}(\vec{\theta}) + b_{ij}(\vec{\theta})$ for channel i and histogram bin j , where s_{ij} represents the potential resonant signal, b_{ij} is the expected background in the bin, and R is a scaling factor applied to the signal.

Systematic uncertainties are parametrized by the de-

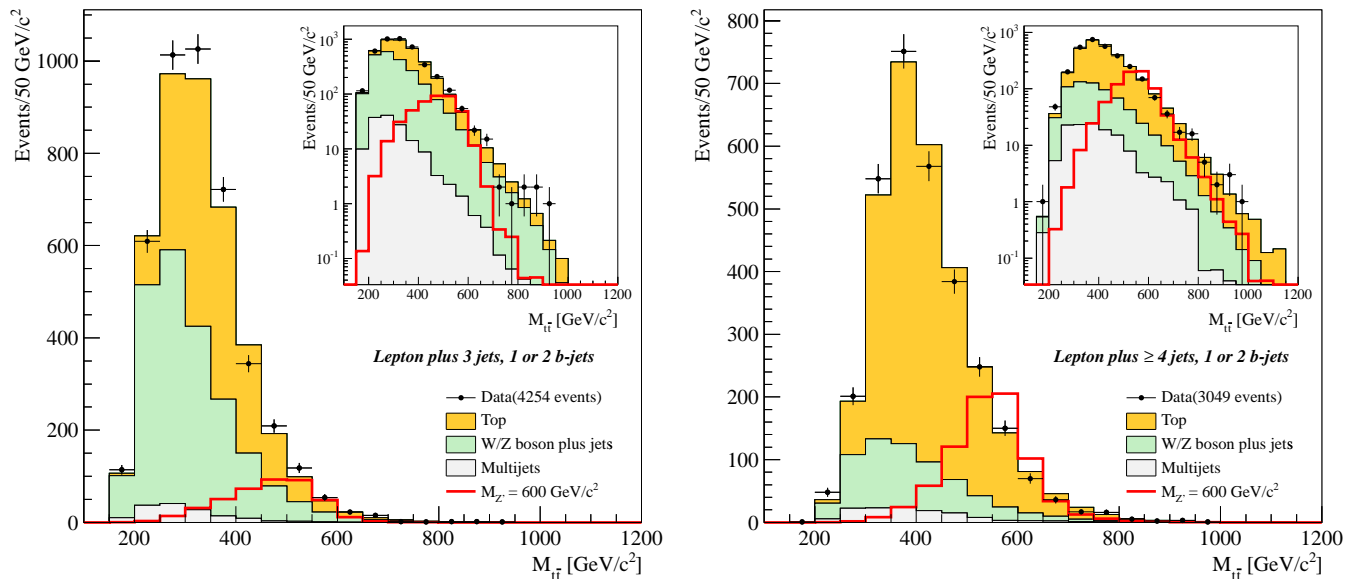


FIG. 1: Reconstructed $M_{t\bar{t}}$ for the three-jet events (left) and four-or-more-jet events (right). The distribution of $M_{t\bar{t}}$ spectrum is on a linear scale and the inset shows a logarithmic scale of the same distribution. The background expectation is normalized to the best fit to the data. The red histogram shows the expectation for a $600 \text{ GeV}/c^2$ mass hypothesis for the leptophobic topcolor resonance normalized to the predicted cross section.

pendence of s_{ij} and b_{ij} on $\vec{\theta}$. Each of the n_{sys} components of $\vec{\theta}$, θ_k , corresponds to a single independent source of systematic uncertainty. We account for correlations by allowing each parameter to have an impact on several sources of signal and background in different channels. Gaussian priors are assumed for the θ_k , which are truncated so that no prediction is negative. The likelihood function, multiplied by the θ_k priors, $\pi(\theta_k)$, is then integrated over θ_k including correlations [11]:

$$\mathcal{L}'(R) = \int \mathcal{L}(R, \vec{s}, \vec{b} | \vec{n}, \vec{\theta}) \pi(\vec{\theta}) d\vec{\theta}. \quad (2)$$

We assume a uniform prior in R to obtain its posterior distribution. The observed 95% C.L. upper limit on R , R_{95}^{obs} , satisfies $0.95 = \int_0^{R_{95}^{\text{obs}}} \mathcal{L}'(\mathcal{R}) d\mathcal{R}$. The expected distribution of R_{95} is computed in an ensemble of pseudo experiments generated without signal. In each pseudo experiment, values of the nuisance parameters are drawn from their priors. The median expected value of R_{95} in this ensemble is quoted as the expected limit. This statistical procedure is repeated for each resonance mass hypothesis from $350 \text{ GeV}/c^2$ to $1200 \text{ GeV}/c^2$.

We consider uncertainties that affect the normalization as well as uncertainties that affect the $M_{t\bar{t}}$ distributions. The same set of uncertainties on the dominant background (SM $t\bar{t}$ production) and the resonant signal are considered: they arise from the uncertainty in the jet

energy scale (JES) [31], the b -tagging efficiency, the luminosity measurement [43], the lepton identification and trigger efficiency, and the rate of initial- and final-state (IFSR) radiation from the parton shower model. The JES, b -tag, and IFSR variations also affect the shape of the $M_{t\bar{t}}$ distributions. The background normalizations for the QCD multijet background and for events with a W boson and heavy-flavor jet (b or c) are assigned uncertainties due to limitations in their data-driven estimations [28]. Uncertainties on the renormalization and factorization scale used in the ALPGEN sample affect the shape of the $M_{t\bar{t}}$ distributions from W boson + jets.

The resulting 95% C.L. upper limits on the cross section times the branching ratio for the leptophobic topcolor Z' [19] signal hypotheses, $\sigma_{Z'} BR(Z' \rightarrow t\bar{t})$, as a function of $M_{t\bar{t}}$ are shown in Fig. 2 and Table II together with expected limits derived from pseudo experiments that include the SM background hypothesis only. A benchmark leptophobic topcolor model [19] is excluded at 95% C.L. for Z' boson masses smaller than $915 \text{ GeV}/c^2$ assuming the width of the resonance is $\Gamma_{Z'} = 0.012 M_{Z'}$. In addition, the limits reported here can be applied to any resonance producing the same final state as long as the decay width is significantly smaller than the reconstruction mass resolution ($\Gamma_{Z'} \ll 0.15 M_{Z'}$).

In conclusion, we have performed a search for a heavy resonance decaying into $t\bar{t}$ using the lepton+jets decay channel in data from 9.45 fb^{-1} of integrated luminosity.

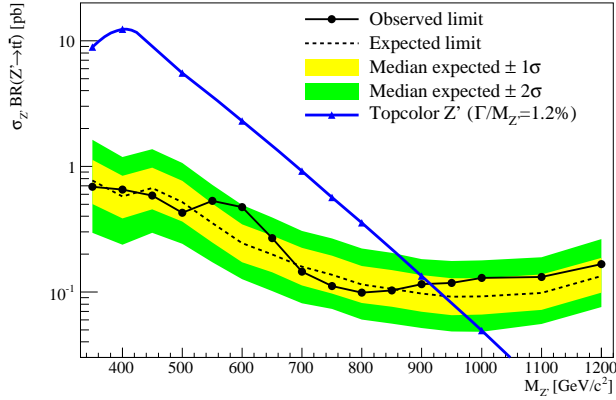


FIG. 2: Expected and observed upper limits on the production cross section times the branching ratio for a leptophobic topcolor Z' boson in 9.45 fb^{-1} of CDF data. The dashed line is the median expected upper limit with the assumption of no signal, the black points are the observed limit, and the blue line is the cross section prediction for leptophobic topcolor Z' boson [19] production.

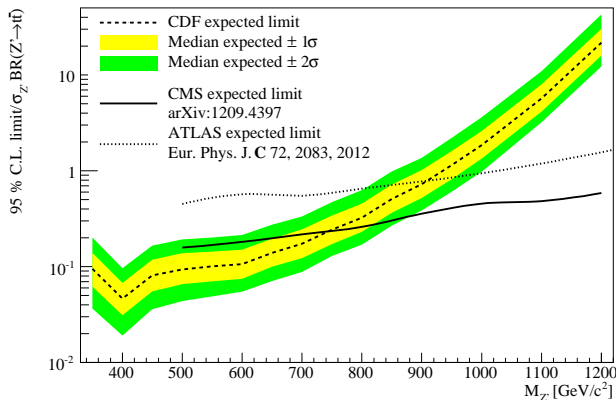


FIG. 3: Tevatron and LHC sensitivity comparison to new physics for narrow $t\bar{t}$ resonant final states, using the benchmark leptophobic topcolor Z' model. The figure shows the expected upper limits on $\sigma_{Z'} BR(Z' \rightarrow t\bar{t})$ divided by the theoretical prediction of $\sigma_{Z'} BR(Z' \rightarrow t\bar{t})$ as a function of $M_{t\bar{t}}$. Dashed, dotted, and solid lines correspond to the expected upper limits of the most sensitive analyses to date from CDF, ATLAS and CMS experiments respectively.

The data are found to be consistent with the background expectation and upper limits are set on the production cross section times branching ratio at the 95% C.L. For a specific benchmark model (leptophobic topcolor), we exclude Z' bosons with masses up to $915 \text{ GeV}/c^2$. As shown in Fig. 3, for masses smaller than approximately $750 \text{ GeV}/c^2$, this search yields the most constraining limits to date on $q\bar{q}$ -produced narrow $t\bar{t}$ resonant states in

$M_{Z'}$ [GeV/ c^2]	Expected [pb]	Observed [pb]	$\sigma_{Z'} BR(Z' \rightarrow t\bar{t})$ [pb]
350	0.772	0.687	8.91
400	0.575	0.652	12.3
450	0.670	0.585	8.24
500	0.520	0.427	5.53
550	0.354	0.530	3.51
600	0.245	0.472	2.30
650	0.199	0.269	1.43
700	0.159	0.145	0.917
750	0.137	0.112	0.566
800	0.115	0.099	0.355
850	0.106	0.103	0.208
900	0.097	0.116	0.134
950	0.091	0.118	0.080
1000	0.092	0.129	0.049
1100	0.098	0.132	0.017
1200	0.134	0.166	0.006

TABLE II: Expected, observed 95% C.L. upper limits and theoretical prediction for the production cross section times the branching ratio for a narrow $t\bar{t}$ resonance, given as a function of Z' boson mass.

the lepton+jets decay mode.

Acknowledgments

We thank the Fermilab staff and the technical staffs of the participating institutions for their vital contributions. This work was supported by the U.S. Department of Energy and National Science Foundation; the Italian Istituto Nazionale di Fisica Nucleare; the Ministry of Education, Culture, Sports, Science and Technology of Japan; the Natural Sciences and Engineering Research Council of Canada; the National Science Council of the Republic of China; the Swiss National Science Foundation; the A.P. Sloan Foundation; the Bundesministerium für Bildung und Forschung, Germany; the Korean World Class University Program, the National Research Foundation of Korea; the Science and Technology Facilities Council and the Royal Society, UK; the Russian Foundation for Basic Research; the Ministerio de Ciencia e Innovación, and Programa Consolider-Ingenio 2010, Spain; the Slovak R&D Agency; the Academy of Finland; and the Australian Research Council (ARC).

- [1] F. Abe *et al.* (CDF Collaboration), Phys. Rev. Lett. **74**, 2626 (1995); S. Abachi *et al.* (D0 Collaboration), *ibid* **74**, 2632 (1995).
- [2] C. T. Hill and S. J. Parke, Phys. Rev. D **49**, 4454 (1994).

- [3] T. Aaltonen *et al.* (CDF Collaboration), Phys. Rev. D **83**, 112003 (2011).
- [4] J. F. Kamenik, J. Shu, and J. Zupan, Eur. Phys. J. C **72**, 2102 (2012).
- [5] V. M. Abazov *et al.* (D0 Collaboration), Phys. Rev. D **85**, 051101 (2012).
- [6] R. Frederix and F. Maltoni, J. High Energy Phys. 01 (2009) 047.
- [7] B. A. Dobrescu, K. Kong, and R. Mahbubani, J. High Energy Phys. 06 (2009) 001.
- [8] M. I. Gresham, I. W. Kim and K. M. Zurek, Phys. Rev. D **83**, 114027 (2011).
- [9] K. Agashe, A. Belyaev, T. Krupovnickas, G. Perez and J. Virzi, Phys. Rev. D **77**, 015003 (2008).
- [10] Y. Bai, J. L. Hewett, J. Kaplan and T. G. Rizzo, J. High Energy Phys. 03 (2011) 003.
- [11] K. Nakamura *et al.* (Particle Data Group), J. Phys. G **37**, 075021 (2012).
- [12] In addition to the 29% branching ratio, tau leptons are included when their decay produces an isolated electron or muon candidate.
- [13] T. Affolder *et al.* (CDF Collaboration), Phys. Rev. Lett. **85**, 2062 (2000).
- [14] T. Aaltonen *et al.* (CDF Collaboration), Phys. Rev. D **77**, 051102 (2008).
- [15] T. Aaltonen *et al.* (CDF Collaboration), Phys. Rev. D **84**, 072003 (2011).
- [16] T. Aaltonen *et al.* (CDF Collaboration), Phys. Rev. D **84**, 072004 (2011).
- [17] C.T. Hill, Phys. Lett. B **345**, 483 (1995).
- [18] R.M. Harris, C.T. Hill, and S.J. Parke, arXiv:hep-ph/9911288.
- [19] R. M. Harris and S. Jain, Eur. Phys. J. C **72**, 2072 (2012), and private communication with the authors.
- [20] V. M. Abazov *et al.* (D0 Collaboration), Phys. Rev. Lett. **92**, 221801 (2004).
- [21] V. M. Abazov *et al.* (D0 Collaboration), Phys. Lett. B **668**, 98 (2008).
- [22] G. Aad *et al.* (ATLAS Collaboration), J. High Energy Phys. 09 (2012) 041.
- [23] G. Aad *et al.* (ATLAS Collaboration), Eur. Phys. J. C **72**, 2083 (2012)
- [24] G. Aad *et al.* (ATLAS Collaboration), arXiv:1211.2202
- [25] S. Chatrchyan *et al.* (CMS Collaboration), J. High Energy Phys. 07 (2012) 029.
- [26] S. Chatrchyan *et al.* (CMS Collaboration), arXiv:1209.4397.
- [27] D. Acosta *et al.* (CDF Collaboration), Phys. Rev. D **71**, 032001 (2005).
- [28] T. Aaltonen *et al.* (CDF Collaboration), Phys. Rev. D **82**, 112005 (2010).
- [29] T. Aaltonen *et al.* (CDF Collaboration), Phys. Rev. D **86**, 032011 (2012).
- [30] F. Abe *et al.* (CDF Collaboration), Phys. Rev. D **45**, 1448 (1992).
- [31] A. Bhatti *et al.* (CDF Collaboration), Nucl. Instrum. Methods Phys. Res., Sect. A **566**, 2 (2006).
- [32] D. Acosta *et al.* (CDF Collaboration), Phys. Rev. D **71**, 052003 (2005).
- [33] F. Sforza, V. Lippi, and G. Chiarelli, J. Phys. Conf. Ser. **331**, 032045 (2011).
- [34] U. Langenfeld, S. Moch, and P. Uwer, Phys. Rev. D **80**, 054009 (2009).
- [35] A. D. Martin, W. J. Stirling, R. S. Thorne, and G. Watt, Eur. Phys. J. C **63**, 189 (2009).
- [36] S. Frixione, P. Nason, and C. Oleari, J. High Energy Phys. 11 (2007) 070.
- [37] T. Aaltonen *et al.* (CDF and D0 Collaborations), Phys. Rev. D **86**, 092003 (2012).
- [38] Torbjörn Sjöstrand, Patrik Eden, Christer Friberg, Leif Lönnblad, Gabriela Miu, Stephen Mrenna, and Emanuel Norrbin, Comput. Phys. Commun. **135** (2001) 238.
- [39] R. Brun, F. Bruyant, M. Maire, A. C. McPherson, and P. Zancarini, CERN Report No. CERN-DD-EE/84-1 (1987) 01.
- [40] G. Grindhammer, M. Rudowicz, and S. Peters, Nucl. Instrum. Methods A **290**, 469 (1990).
- [41] M. L. Mangano, M. Moretti, F. Piccinini, R. Pittau, and A. D. Polosa, J. High Energy Phys. 07 (2003) 001.
- [42] J. Gao, C. S. Li, B. H. Li, C. -P. Yuan, and H. X. Zhu, Phys. Rev. D **82**, 014020 (2010), and private communication with the authors.
- [43] S. Klimenko, J. Konigsberg, and T. M. Liss, FERMILAB-FN-0741 (2003).